Engineering Structures 243 (2021) 112551

Contents lists available at ScienceDirect

Engineering Structures

journal homepage: www.elsevier.com/locate/engstruct

Testing of a full-scale flat slab building for gravity and lateral loads

Dario Coronelli [a], Marco Lamperti Tornaghi [b,*], Luca Martinelli [a], Francisco-Javier Molina [b], Aurelio Muttoni [c], Ion Radu Pascu [d], Pierre Pegon [b], Marco Peroni [b], António Pinho Ramos [e], Georgios Tsionis [b], Teresa Netti [a]

[a] Politecnico di Milano, Department of Civil and Environmental Engineering, 20133 Milano, Italy
[b] European Commission, Joint Research Centre (JRC), 21027 Ispra, Italy
[c] École Polytechnique Fédérale de Lausanne, 1015 Lausanne, Switzerland
[d] Universitatea Tehnică de Construcţii Bucureşti, 020396 Bucureşti, Romania
[e] Universidade Nova de Lisboa, Department of Civil Engineering, 2829-516 Caparica, Portugal

ARTICLE INFO

Keywords:
Flat plate
Full-scale testing
Pseudo-Dynamic Testing
Seismic and cyclic loading
Punching shear
Hybrid Simulation

ABSTRACT

Full-scale testing of a two-storey flat slab structure is reported, undertaken in the SlabSTRESS research project; the construction and testing were planned and carried out at the ELSA laboratory of the European Commission's Joint Research Centre. The dimensions are three bays by two, spans 4.5 and 5 m, slab thickness 0.2 m, interstorey height 3.2 m. Two different longitudinal reinforcement details were considered; welded studs shear reinforcement was provided only in the second floor slab. The testing program included seismic tests for service and ultimate actions, using the pseudodynamic technique with virtual walls. To this aim a building structure was designed with primary walls and the flat slab frame as secondary element. Cyclic loading tests followed up to ultimate drift capacity of the structure. The sequence of tests included strengthening of a set of damaged connections using bolted bars in holes drilled through the slab, followed by cyclic testing to failure. The instrumentation was provided for the global response and the connections with local rotations in the columns and slab; cracking around the columns was measured with through-crack sensors; a measurement system for internal forces and moments was included within the columns. The results show the response with deformations and damage for the different loading conditions up to failure. The results obtained on a full-scale structure extend and confirm the knowledge in the literature, mainly based on isolated connections and/or small-scale samples.

1. Introduction

Flat slabs are one of the most common solutions for building floors worldwide, including seismic countries. In the Eurocode pre-normative documents [1] flat slabs are defined as two-way slabs with constant thickness or drop panels. The knowledge of the structural behaviour for combined lateral and gravity loads is based mainly on small scale specimens or sub-assemblies, most of which slab-column connections. Complementary real scale experimental studies on flat slab structures are needed. A review and synthesis of test results on connections can be found in Hueste et al. [2], Zhou et al. [3] and Ramos et al. [4]. The tests in the literature concern mainly internal columns. Different punching and flexural failure modes are shown. The results show the effect of different parameters such as column size, slab thickness, amount and layout of longitudinal reinforcement, use of transverse reinforcement. For internal columns, the ultimate drift ratio has been correlated to the *Gravity Shear Ratio* (GSR), the ratio between the effects of gravity loads and punching shear strength to provide models for the design of flat slab frames based on the drift ratio. A state of the art for floor and frame tests has been reported in Coronelli et al. [5]. Tests on floor specimens with scaled dimensions were carried out with cyclic actions by Hwang and Moehle [6,7] and Rha et al. [8]. Shaking table tests on two storey flat slab frames were conducted by Moehle and Diebold [9] and Kang and Wallace [10,11]. The scale factors range between 30% and 50%. Fick et al. [12] tested a full scale three storey building. The floor and frame tests provide results also for edge and corner connections. The tests considered *Gravity Shear Ratios* (GSR) for internal columns between 0.2 and 0.3, with only one study with GSR = 0.4 [8]. Only one specimen

* Corresponding author.
E-mail address: marco.lamperti-tornaghi@ec.europa.eu (M. Lamperti Tornaghi).
URL: https://www.slabstress.org/ (D. Coronelli).

https://doi.org/10.1016/j.engstruct.2021.112551
Received 30 October 2020; Received in revised form 19 April 2021; Accepted 13 May 2021
Available online 18 June 2021

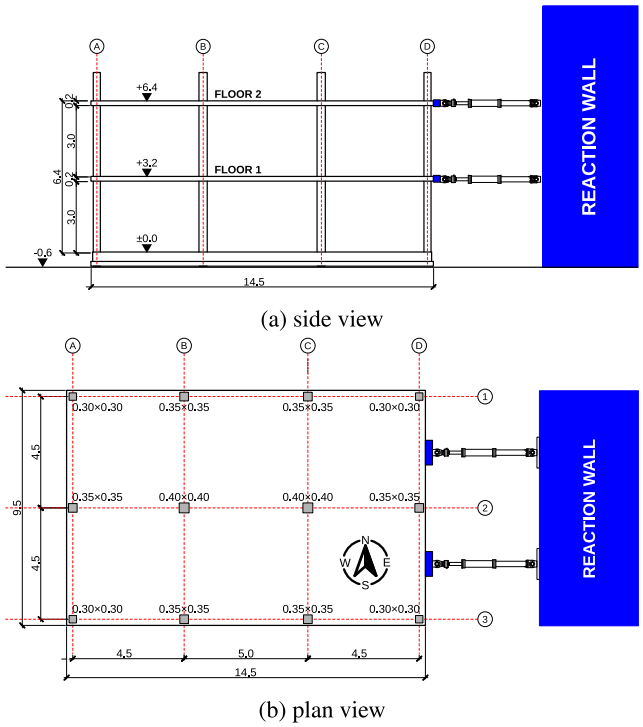

Fig. 1. Side (a) and plan (b) view of the building.

Table 1
Concrete Testing (cubes).

Structural elements	f_c (MPa)	R_c (MPa)	st.dev (MPa)	samples n.
Foundation	23.2	27.9	±3.5	4
Columns (1st floor, lower half)	14.9	17.9	±0.5	2
Columns (1st floor, top half)	27.9	33.6	±0.1	2
Slab (1st floor)	33.0	39.7	±0.2	3
Columns (2nd floor)	38.0	45.8	±3.2	4
Slab (2nd floor)	35.6	42.9	±1.6	3

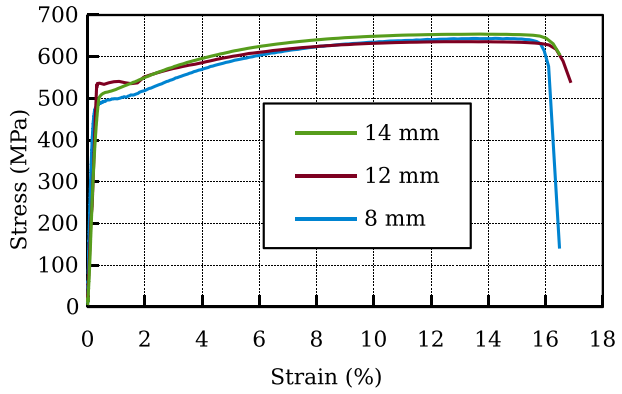

Fig. 2. Material characterisation of slab-reinforcement steel bars.

considered transverse reinforcement along with conventional longitudinal rebars [10]. Results on the ultimate drift ratio related to the GSR broadly agree with those obtained on connections, considered that there is a lot of scatter in the results, for the range of GSR considered. As mentioned above, only one test in the literature studied a full scale three storey flat slab frame [12]. The slab thickness was 180 mm, the spans were 6.1 m, with 1.5 m overhangs around all columns. The structure was designed for gravity loading only; the GSR was 0.21 in the internal connections. The first punching failure occurred at 3.3% drift ratio (top displacement divided by building height), after which the test was stopped. The experimental set-up did not include the measurement of the actions in each connection. The brief summary of experimental research given above shows that more full scale tests are needed, with realistic boundary conditions and taking into consideration dimensions in common use. The design of the structure should consider lateral actions. The tests should study the whole response, exploring ultimate conditions as far as possible in relation to the testing facilities [5]. The main aim of the research presented in this paper is to provide experimental evidence for the response of flat slab frames and buildings under combined gravity and lateral loads. The SlabSTRESS project (Slab Structural RESponse for Seismic design, www.slabstress.org) was launched by a group of European universities, led by the *Politecnico di Milano* together with the EPFL (*École Polytechnique Fédérale de Lausanne*), UNOVA (*Universidade NOVA de Lisboa*) and UTCB (*Universitatea Tehnică de Construcţii Bucureşti*), in collaboration with the Joint Research Centre of the European Commission. The research studied a real scale flat slab structure constructed and tested at the reaction wall facility of the ELSA laboratory of the European Commission's Joint Research Centre in Ispra, Italy. This paper presents the testing program carried out on the two storey specimen and the results obtained. The tests include the seismic response of the flat slab frame coupled with walls and the cyclic response of the flat slab frame. The seismic tests investigated the response and damage to accelerograms compatible with the *serviceability* and *ultimate limit state* (SLS and ULS) earthquake action. Pseudodynamic testing with numerically modelled walls was used. The cyclic quasi-static tests studied the global response for gravity and lateral loading, with the response of different types of connections from the initial behaviour to failure; the redistribution of load effects in the floors and the building; the efficiency of different reinforcement details proposed in Eurocode 2 (EC2) [13] or used in practice; the adequacy of a repair and retrofit system. The testing of the building complements and completes the knowledge of experiments on isolated slab-column connections, giving information about the stiffness and deformation capacity of these structural systems [5]. Floors are structural systems exhibiting a redistribution of internal forces amongst the different interior, edge and corner connections that has to be studied in order to achieve adequate deformation capacity of the whole structure. The testing of a whole frame allows considering realistic boundary conditions on the critical zones in the slab close to the columns and the membrane effect of the slab. Full-scale testing considers size-effect in specimens of realistic dimensions. A further aspect considered is the role of transverse reinforcement, for which limited research was carried out by previous tests of floors and frames. The second floor slab was provided with welded studs. After an initial cyclic test, strengthening of some slab-column connections on the first floor was carried out using post-installed bolted bars. This issue is of particular relevance for the maintenance and retrofitting of existing structures. The experimental setup includes measurement of global displacements and forces; rotations of the columns and rotations of the slab in points close to the columns; crack openings across the thickness of the slab. An innovative system was designed and used for the measurement of column internal forces and moment at each floor of the structure. The first following section describes the specimen, the test setup and testing program are then presented. The results are reported for the seismic tests first and then for the cyclic tests. The main findings are discussed, and conclusions with future developments and research outlooks are proposed. Given the space limitations, the paper reports the global results recorded during the experimental campaign with few local data. A more in-depth analysis of the local results, including the data acquired by the instrumentation installed on the individual connections, will be provided in a further paper.

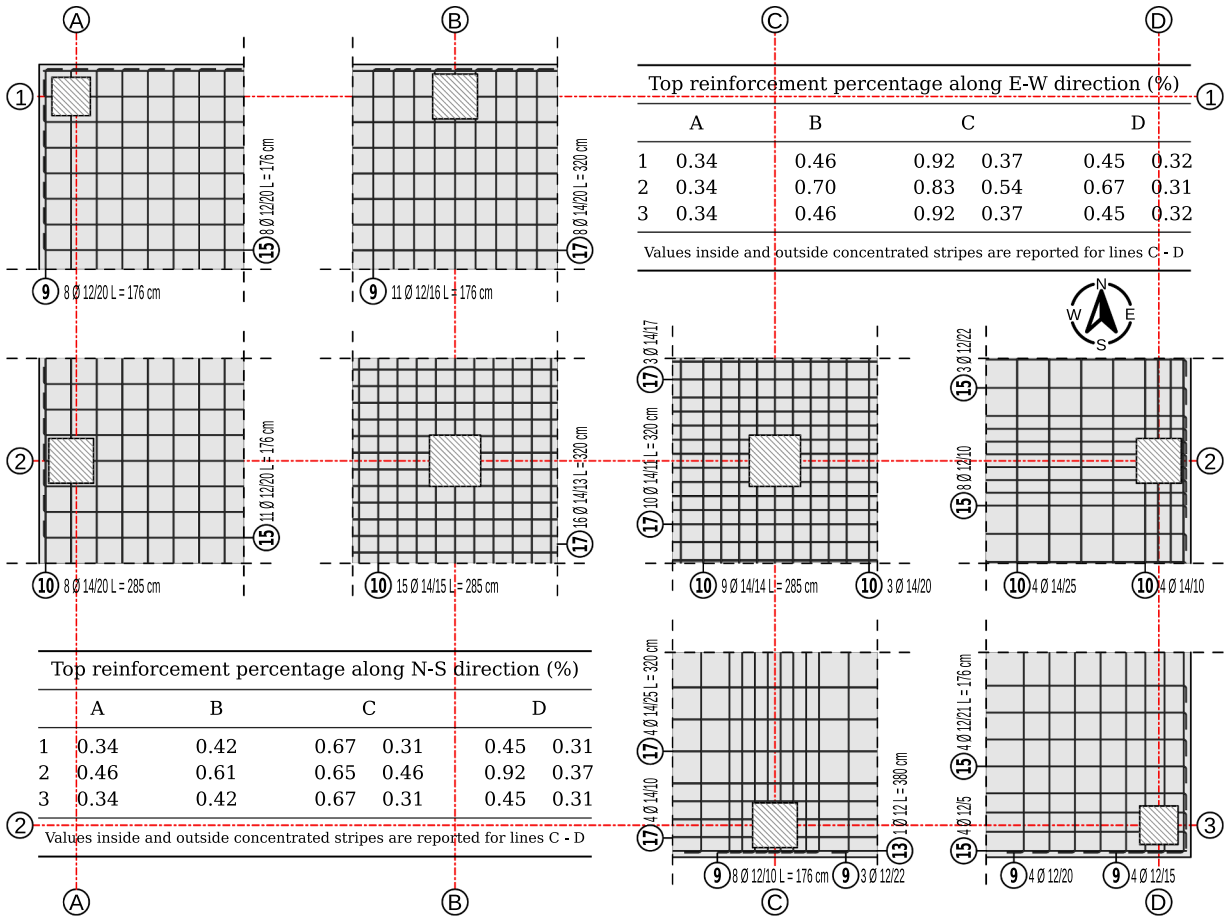

Fig. 3. Top longitudinal reinforcement in the slab around columns.

2. SlabSTRESS Test specimen

2.1. Description of the specimen

The structure is a two floor flat slab frame, with three by two bays, shown in Fig. 1a and 1b. The floors are ordinary reinforced concrete slabs 0.2 m thick. The spans are 4.5 m and 5 m in the longitudinal direction and 4.5 m in the transverse direction. The storey height is 3.2 m. Columns cross sections are square with dimensions 0.4, 0.35 and 0.3 m for internal, edge and corner columns respectively. The presence of walls for the pseudodynamic testing was simulated as explained in Section 3.

The concrete properties measured on cubes during the construction are reported in Table 1. The rebars used in the floor slabs and foundation is B450C (characteristic steel yield strength f_{yk} = 450 MPa), see Fig. 2. In the columns, S500 Class B reinforcing steel (f_{yk} = 500 MPa) was used, with the exception of the column bases, where B450C is placed. The steel yield strength of the punching reinforcement studs was f_{yk} = 500 MPa.

The slab longitudinal reinforcement was designed according to Eurocode 2 specifications (see Section 2.2). The longitudinal reinforcement in the top layers at the slab-column connection (Fig. 3) was detailed according to two patterns: *smeared* and *concentrated* reinforcement. The latter was obtained with half of the total reinforcement for the support section in a quarter of the section width, as recommended in EC2 [13]. The connections along lines A and B had smeared reinforcement, while along lines C and D there was concentrated reinforcement. Two bottom bars in each direction were placed at each connection, following another detailing rule in EC2 [13]. The anchorage at the slab free edge was a L-shaped bend of length 40 times the rebar diameter, as commonly used in the European practice.

On the basis of the gravity loading design (see the following Section 2.2), the slab-column connections at the first floor were not reinforced against punching shear. The second floor slab was reinforced using headed studs as punching shear reinforcement (Fig. 4a). Though not required by the gravity load design, this choice was made to test the performance of slab-column connections of different configurations (interior, edge and corner and two flexural reinforcement layouts) when punching shear reinforcement is used in a flat slab with realistic thickness. Given the economic investment for the test and the chance to test only one structure, the choice was made to use shear studs in only one of the floors.

After a first testing phase with significant inter-storey drift ratios, which produced damage on the slab-column connections, the connections B1-1, C2-1 and C3-1 on the first floor were strengthened using post-installed bolts using the same layout of the pre-installed studs. The purpose of strengthening the connections was to verify the effectiveness of post-installed bolts in connections damaged by earthquake of a complete full-scale structure with realistic dimensions. Further details are given in Section 6.2.

2.2. Design of the test building

The seismic design of the structure was carried out as a secondary flat slab frame in a building with primary seismic resistant walls. The design procedure here summarised complies with Eurocode 8 (EC8) [14] provisions for primary and secondary elements. The building was designed for a zone of moderate-high seismicity. The design drift ratio was relatively low, equal to 0.4%, for reasons further explained below. The design was carried out for the ultimate and service state seismic situations, and gravity ultimate limit state. The Italian code NTC 2018 [15] was used, compatible with Eurocode 2 [13] and 8 [14] provisions; for

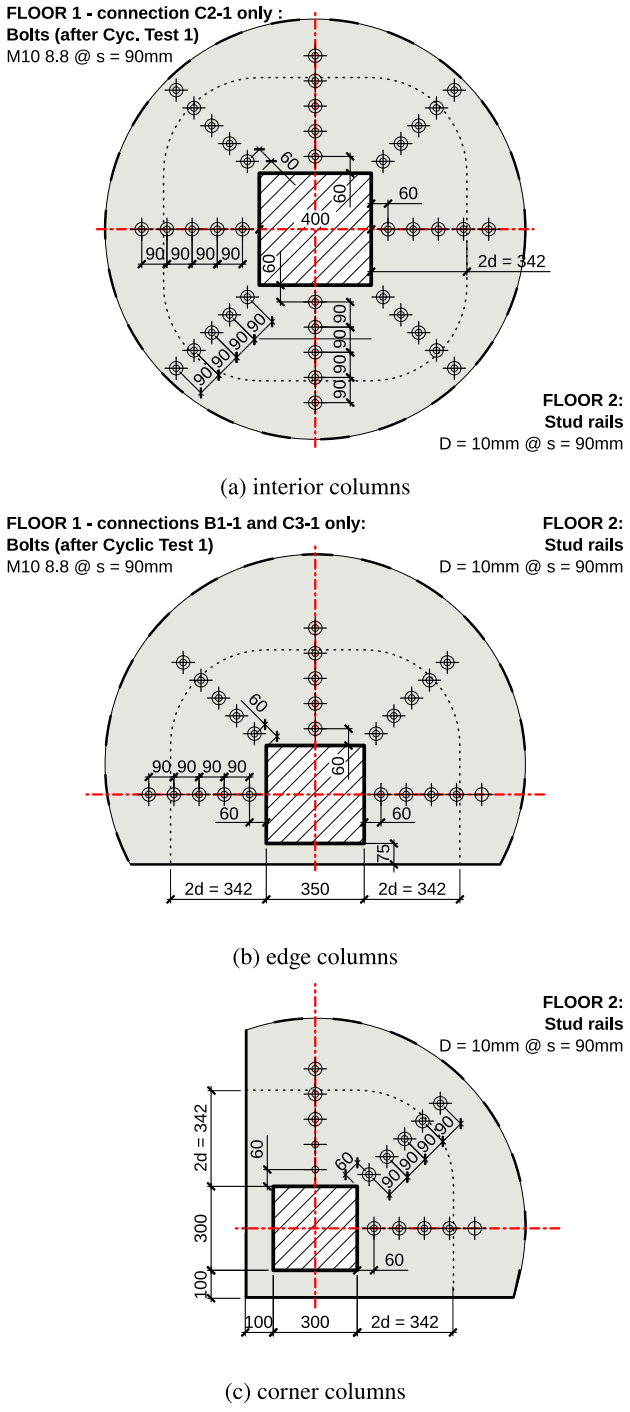

Fig. 4. Layout of punching shear reinforcement of slab-column connections at the second floor (stud rails d = 10 mm @ 90 mm) and at first floor after test CYC-1 (bolts M10 8.8); *d* is the mean effective depth of the slab.

aspects of flat slab design not covered in NTC08, the code itself proposes the use of EC2 [13]. The seismic Ultimate Limit State (ULS) design action considered the behaviour factor (q = 4) for wall systems. The loads and spans were chosen in relation to common choices in residential buildings and for the some dimensions in relation to space limitations in the laboratory. The preliminary design of the flat slab in the interior connections was carried out to obtain a gravity shear ratio (ratio of the gravity load effects in the seismic situation to the punching shear resistance) equal to 0.3. This choice was made to provide deformation capacity to the connections with the development of nonlinear deformations (Pan and Moehle [16]; Hueste et al. [2]; Ramos et al. [4]; Drakatos et al. [17]). In Eurocode 8 [14] design of a system with primary and secondary elements, the former take the seismic action; the latter should bear the gravity loads up to the deformations reached by the primary system. In addition the cracked stiffness of the secondary elements should not be more than 15% of that of the primary elements. Slender ductile primary walls were designed accordingly, using the codes indicated previously. This resulted in the dimensions given in 2.1 and low deformations for the given seismic actions. The design of the flat slabs for the seismic situation was carried out as follows. The limitation on the gravity shear ratio of the connections was used to guarantee that the secondary elements would bear the gravity loads at the deformations of the primary system. The drift capacity was estimated based on the existing results in the literature (Pan and Moehle [16]; Hueste et al. [2]; Zhou and Hueste [3]; Ramos et al. [4]). The ULS deformations of the primary elements were calculated with a cracked stiffness and for the ULS seismic action, multiplied by q = 4. These were verified to be smaller than the drift capacity. In addition, the seismic action effects for the seismic situation in the slab were calculated and compared to the gravity ULS load effects; the latter resulted to be the dominating combination of actions. The slab longitudinal reinforcement and punching shear design were carried out according to EC2 [13]. As already mentioned, the verification showed that shear reinforcement was not required. The columns design was carried to obtain a column resistance in the cross sections framing into the slab greater than the effects of the maximum possible moment transfer from the slab. The latter was determined on the basis of the slab geometry and reinforcement using the proposal by ACI 421-07 [18]. The same longitudinal reinforcement was used along the whole length of the members, with the exception of the connection to the foundations. Here the resistance was chosen to be equal to the moment effect of the conditions described above. This resulted in a reinforcement ratio at the base of the column lower than in the parts in elevation. The aim of this procedure was to force the formation of plastic hinges at the columns bases in the cyclic tests, planned to reach high lateral deformations. The transverse reinforcement in these cross-sections was detailed accordingly.

Table 2
Test programme.

#	Test id.		Type of test	Maximum action
	ext.	int.		
1	SEIS-SLS	e03	PsD	SLS (PGA = 0.884 m/s^2)
2	SEIS-ULS	e06	PsD	ULS (PGA = 2.498 m/s^2)
3	CYC-1	f02	Cyclic	2.5% drift ratio
4	CYC-2	g04	Cyclic	6.0% drift ratio

PsD: Pseudo-Dynamic Test, see 3.1.
PGA: Peak Ground Acceleration, see 3.1.

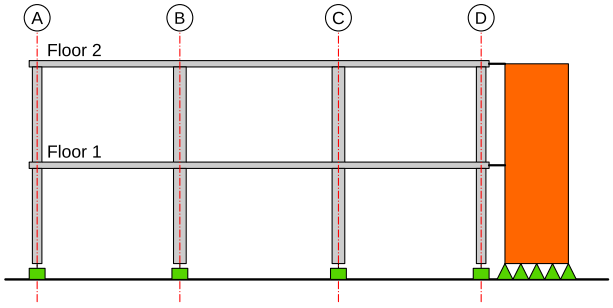

Fig. 5. Conceptual scheme of the building.

3. Test programme

The aim of the SlabSTRESS experimental campaign was twofold: first

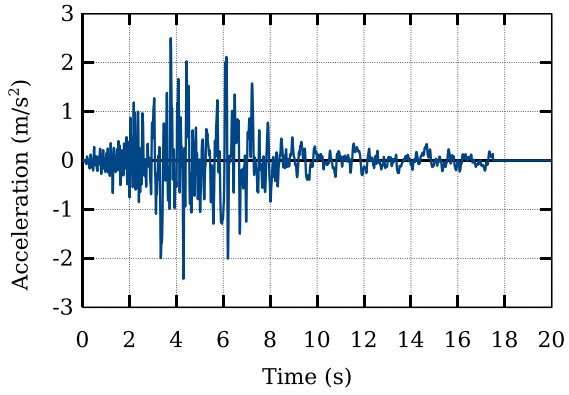

(a) time-history of the selected accelerogram for test SEIS-ULS

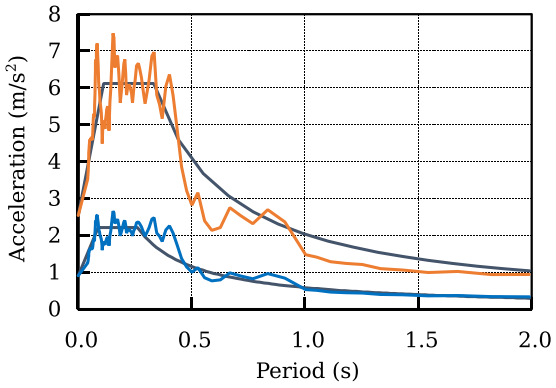

(b) Pseudo-acceleration response spectra of the input accelerogram and design spectra at SLS (blue line) and ULS (red line)

Fig. 6. Inputs of seismic tests.

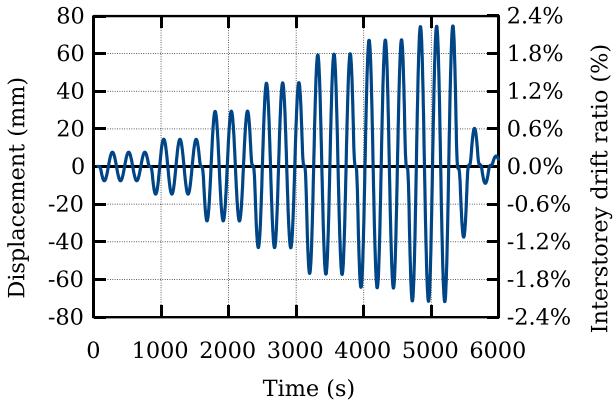

(a) Tests CYC-1

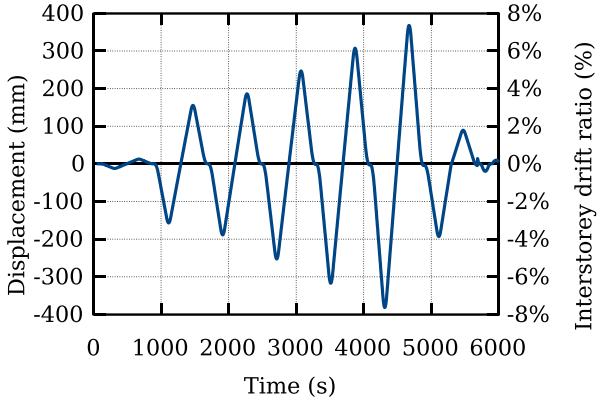

(b) Tests CYC-2

Fig. 7. Global drift ratio history for tests CYC-1 and CYC-2.

to verify the seismic performance of a structure designed according to the procedure in the previous section, with ductile walls and flat slab frames as primary and secondary seismic members respectively, and secondly to study the performance of the flat slab frame beyond the design displacements (Table 2). Pseudo-dynamic tests were performed first on the specimen treated as part of a building with two numerical shear walls (Fig. 5) to study its seismic performance at the Serviceability (SEIS-SLS 5.1) and Ultimate Limit States (SEIS-ULS 5.2). Test SEIS-ULS aimed into verify the requirement of the EC8 [14] that the flat slab frame maintains the capacity to bear gravity loads when subjected to the maximum deformations reached for the seismic design action. Quasi-static tests were subsequently performed on the specimen – without the numerical shear walls – subjected to cyclic loading with increasing displacements. The test sequence was planned to achieve a progressive and controlled damage of slab-column connections. Test CYC-1 (6.1) aimed to study the cyclic response of the flat slab frame until punching shear failure was observed at the first floor. Test CYC-2 (6.3) was performed after a set of the slab-column connections of the first floor were strengthened (6.2).

3.1. Seismic test

The input ground motion for the seismic tests was the Y component of signal 00712ya recorded during the M_W 6.4 Bingöl earthquake of 1 May 2003. The original $PGA = 2.92$ m/s^2 was scaled at 31% and 87% for tests SEIS-SLS and SEIS-ULS respectively to match the Eurocode 8 [14] elastic spectra for the SLS and ULS. Fig. 6a shows the acceleration time history used in test SEIS-ULS together with the pseudo-acceleration response spectra of the selected accelerogram and the design spectra of EC8 at SLS and ULS, Fig. 6b. Furter details about seismic tests are provided in the appendix A.

3.2. Cyclic test

A displacement history was imposed on the second floor and half of the measured horizontal force at the second floor was imposed on the first one for tests CYC-1 and CYC-2. For test CYC-1, the displacement history at the second floor was made up of sets of three cycles with increasing values of global drift ratio (top floor displacement/building height): 0.25%, 0.5%, 1%, 1.5%, 2%, 2.25% and 2.5% (Fig. 7a). Test CYC-2 was performed for single cycles of global drift ratio 2.5%, 3%, 4%, 5% and 6% (Fig. 7b).

4. Test set-up

4.1. Loading system

The horizontal displacement on each building floor was imposed by a pair of hydraulic actuators connected to the ELSA reaction wall and aligned along the North–South direction. Each jack had a stroke of ± 500 mm and a working load of ±500 kN, for a total load capacity of 2000 kN. All the actuators were equipped with a load cell mounted on the piston rod, which measured the force transferred to the structure through a steel beam placed in the centreline of each bay and connected to the slab with preloaded bolts. The horizontal displacement at each floor level was continuously measured by four high-resolution (2 μm) displacement transducers placed along the E-W load line. These Heidenhain optical encoders were mounted on two reference frames and provided feedback to the PID controller of each actuator.

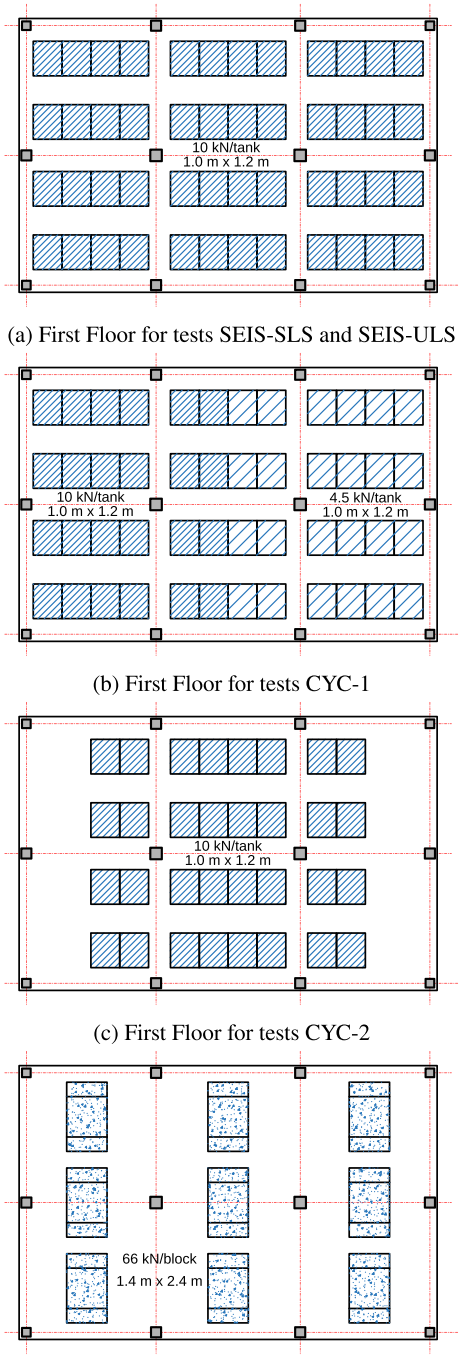

(a) First Floor for tests SEIS-SLS and SEIS-ULS

(b) First Floor for tests CYC-1

(c) First Floor for tests CYC-2

(d) Second Floor for all tests

Fig. 8. Layout of additional gravity loads.

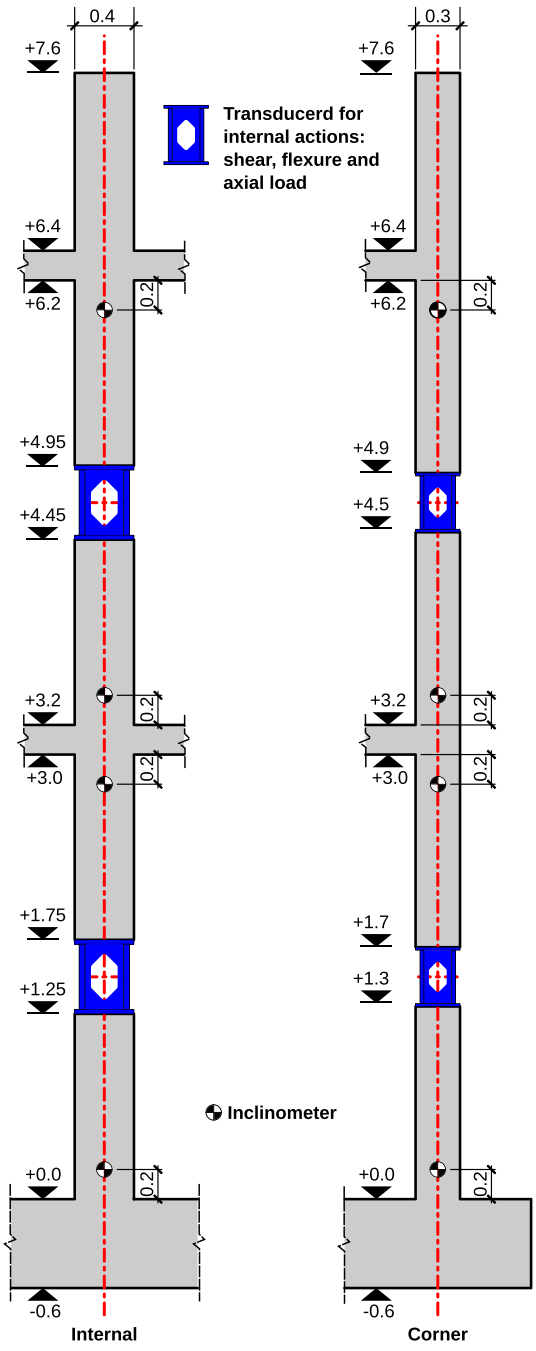

Fig. 9. Layout of internal action measurement devices and column inclinometers.

Table 3
Additional vertical loads (kN/m^2).

Test id.	Floor 1		Floor 2	
	East	West	East	West
SEIS-SLS	3.5	3.5	4.3	4.3
SEIS-ULS	3.5	3.5	4.3	4.3
CYC-1	1.5	3.5	4.3	4.3
CYC-2	0*/3.5*	0*/3.5*	4.3	4.3

(*) half of the A-B and C-D spans had no additional load.

4.2. Gravity load

In addition to the self-weight of the flat slab frame, water tanks and concrete blocks were placed on the first and second floor respectively to impose vertical loads reproducing distributed loads, according to the scheme shown in Fig. 8.

SEIS-SLS and SEIS-ULS tests employed 3.5 kN/m^2 additional loads on the first floor (Fig. 8a and 4.3 kN/m^2 on the second floor (Fig. 8d). In the first cyclic test (CYC-1), two values of vertical loads were used respectively for the West and East side of the first floor: 3.5 kN/m^2 and 1.5 kN/m^2 (see Fig. 8b). In the second cyclic test, a load of 3.5 kN/m^2 had to be evenly distributed on the West and East side of the first floor. Since the slab-to-column connections along the A and D lines of the first floor were heavily damaged during the CYC-1 test (see Section 6.1), the outer

Table 4
Instrumentation.

Purpose	Instrument type	Full-scale	n. devices
Slab crack open.	Lin. Displ. Tran.	±5 deg	48
Slab rotation	Inclinometer	±5 deg	48
Column rotation	Inclinometer	±5 deg	32
Shear load	Wheatstone br.	40÷150 kN[1]	24
Bending moment	Wheatstone br.	80÷300 kNm[1]	24

[1] Load cells are different for internal, edge and corner columns

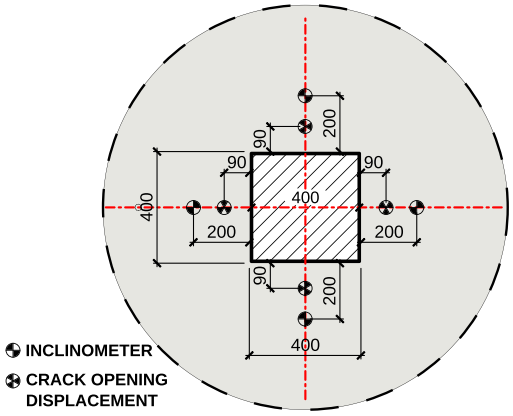

(a) interior columns: B2 and C2

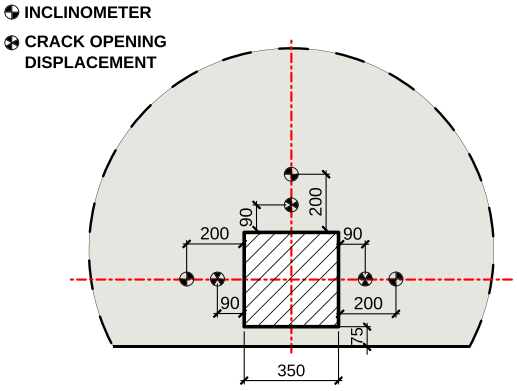

(b) edge columns: B1 and C3

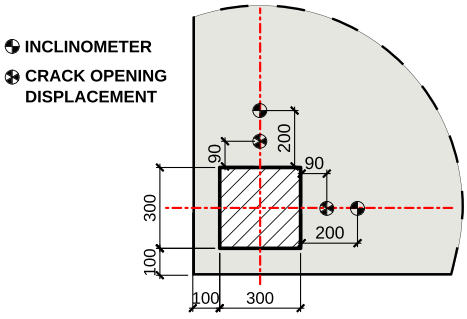

(c) corner columns: A1 and D3

Fig. 10. Layout of instruments on the slab-column connection: inclinometers and crack opening through the variation of slab thickness.

halves of the spans between A and B and between C and D were not loaded during the CYC-2 test as represented in Fig. 8c. The vertical loads on the second floor were the same for all tests. Table 3 summarises the corresponding values of uniform loads for all tests.

Fig. 11. Mock-up setup prior to the tests (North East view).

4.3. Transducers for local measurements

Internal actions (shear force and bending moment) in all columns at both floors were measured using ad hoc internal transducers (Fig. 9a). The transducers for measuring the internal actions were placed at the mid-height of the columns during the construction of the specimen and the strain gauges were installed afterwards. For this reason, they were not calibrated individually, but a calibration of two identical samples for each type of transducer (for interior, edge and corner columns) was performed according to a special calibration procedure the procedure will be described in a following paper. Each type of load cell has its own full scale, as specified in the Table 4.

A reduction of the measure points for rotations and crack openings was allowed by the double-symmetry of the mock-up. Therefore, local kinematic measurements were performed on eight out of the twelve columns and in the surrounding area of the slabs. The rotations along the loading direction were measured both at column top and bottom. The three types of column-slab connections (interior, edge and corner) were analysed with four, three and two instrumented sides respectively. Each side of column-slab connection was equipped with an inclinometer to measure the slab rotation along the E-W direction, and a set of potentiometers to measure crack widths through the slab thickness, as in Fig. 10. The clusters of instruments for the interior columns B2 and C2 had therefore 26 signals each (Fig. 10a), for the edge columns (A2, B1, C3, D2) 22 signals each (Fig. 10b), and finally the corner columns (A1 and D3) 18 signals each (Fig. 10c). A summary of the instrumentation is presented in Table 4. All measurements were digitally converted and grouped in clusters and the data was routed through the local network to the data acquisition server. Each kinematic measuring device was calibrated on a measuring bench before it was placed on the specimen. An analysis of these local measurements cannot be provided here for space constraints.

The experimental set-up is completed with some passive safety measures, designed to avoid catastrophic failures caused by unforeseen events during the tests. These measures included safety bracing along the A and D alignments (West and East side); fall protection systems, i.e. props on the lower floor and metal capitals on the upper floor. All these systems were designed to be activated only in case of emergency, while they did not alter the structural behaviour of the mock-up under normal conditions, see Fig. 11.

5. Seismic tests results

The seismic Tests SEIS-SLS and SEIS-ULS were carried out with the PsD technique, see Appendix A. Test SEIS-SLS adopted a ground motion compatible with the NTC2018 [15] response spectrum at the Damage Limit State (DLS), while test SEIS-ULS a ground motion compatible with

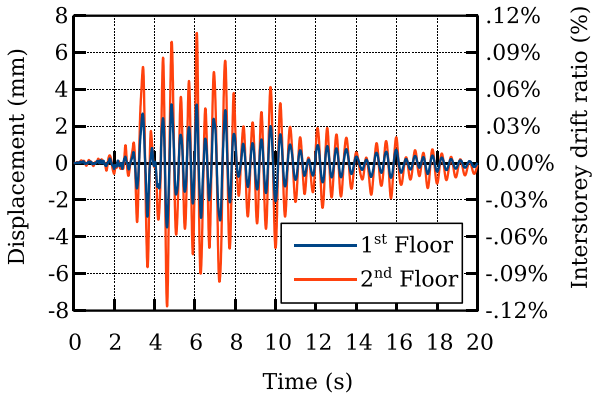

(a) Test SEIS-SLS, lateral displacements.

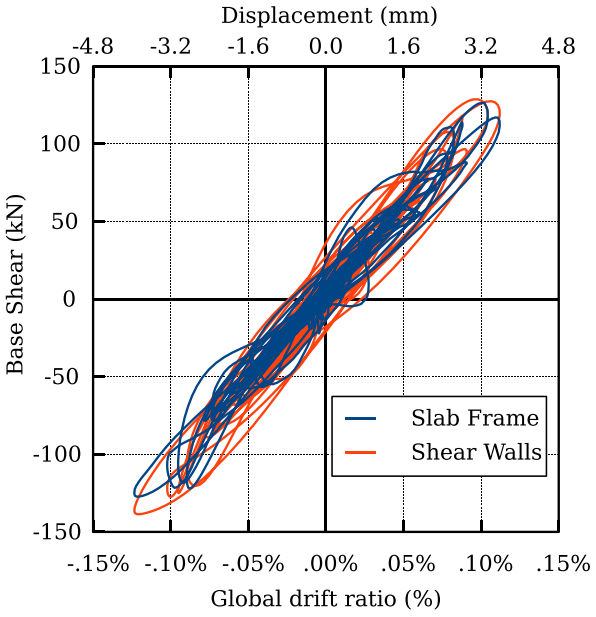

(b) Test SEIS-SLS, base shear force versus global drift ratio.

Fig. 12. Global building response during the test SEIS-SLS.

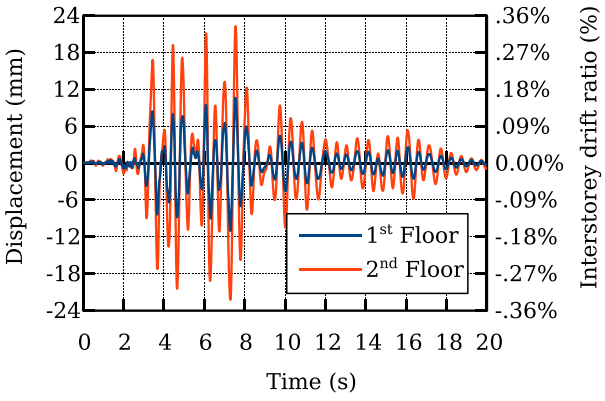

(a) Test SEIS-ULS, lateral displacements.

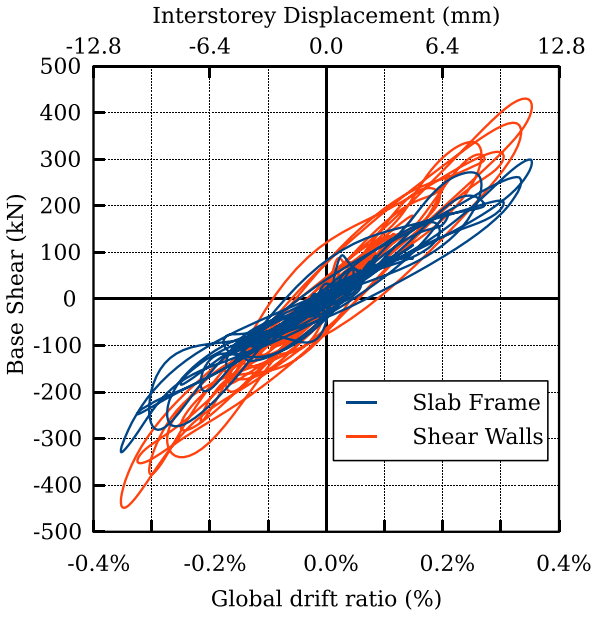

(b) Test SEIS-ULS, base shear force versus drift ratio.

Fig. 13. Global building response during the test SEIS-ULS.

the Life Safety Ultimate Limit State (previously shown in Fig. 5), which is the limit state equivalent to the Ultimate Limit State in Eurocode 8 [14].

5.1. Seismic test SEIS-SLS

The storeys lateral displacements for test SEIS-SLS are reported in Fig. 12a. The maximum recorded values from the test were 0.1% for Level 1 and 0.13% for Level 2, in line with the expectations and well within the 0.5% limit for buildings having brittle non-structural elements attached to the structure, prescribed as acceptable by the design code at the DLS. With these low values basically no significant crack opening in the slab took place. The maximum recorded values on the West and East sensors were close to 0.5 μm at Level 1 and Level 2 but for a few sensors. The West sensor next to column B2 at Level 1 (B2-1) showed regular symmetric cycles of increasing amplitude, with similar maximum positive and minimum negative values of about 0.8 μm in absolute value. The East sensor of column C2-1 showed racketing reaching a maximum negative amplitude of 18 μm. The East sensor for connection A1-2 showed regular symmetric cycles of maximum amplitude 12 μm.

The seismic response in terms of the resultant of restoring forces (shear force at the base) versus drift ratio (displacement of top floor/ total height) is reported in Fig. 12b for the walls and the flat slab frame (the walls, being linear, include both elastic and viscous contributions). The response is almost linear, with an average stiffness of the flat slab frame of about 21977 kN/m. This is in line with the results of an elastic linear model without stiffness reduction for columns and slabs: 21693 kN/m. A small hysteretic damping is present in the test for the flat slab frame (equivalent damping factor below 1.9% with respect to the critical one in the cycle with maximum amplitude, at time 4.608 s). This value of damping is associated in RC structures to very low vibrations levels that do not induce a substantial damage (e.g. human induced vibrations due to walking). These results confirm an essentially linear behaviour.

5.2. Seismic test SEIS-ULS

The storeys lateral displacements for test SEIS-ULS are reported in Fig. 13a, while the seismic response in terms of the resultant of restoring forces (shear force at the base) versus drift ratio (displacement of top floor/ total height) is reported in Fig. 13b. The design values of interstorey drift for this test were 0.25% at the first storey (Level 1) and 0.42% at the second (Level 2). The recorded values from the test where 0.34% for Level 1 and 0.36% for Level 2. The almost equal interstorey drift ratio at the two levels reflect the frame-wall interaction, absent in the design values since they were computed according to the Eurocode 8

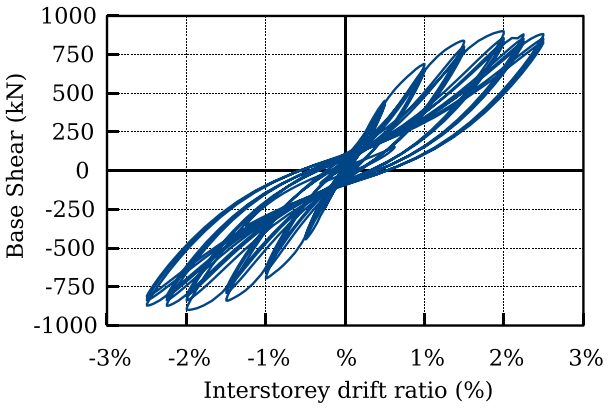

(a) Base shear vs global drift ratio.

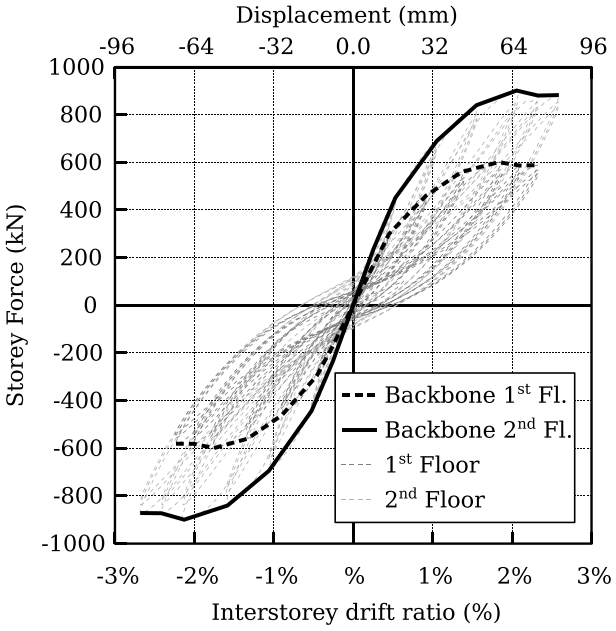

(b) Storey forces as a function of inter-storey drift ratio.

Fig. 14. Global building response during the test CYC-1.

[14] specifications considering the seismic primary members only (the walls), with a factored stiffness (50% of the gross section stiffness) as suggested by the code. As Fig. 13b points out, the flat slab frame part showed a stiffness comparable to that of the walls, the average stiffness is 14514 kN/m for the flat slab frame part and 21186 kN/m for the walls, with the slab providing about 40% of total stiffness. Since in Test SEIS-SLS the stiffness of the flat slab frame was 21977 kN/m, the stiffness for test SEIS-ULS is about 66% with respect to that of test SEIS-SLS. This reduction is consistent with the initial slab cracking for an elastic model of the flat slab frame with no stiffness reduction for the column and a 50% reduction for the slabs gave a numerical value of 15416 kN/m, compared to the experimental value of 14514 kN/m reported above. In spite of the larger values of displacements attained in the second test, an essentially linear behaviour can still be assumed. The hysteretic damping in the cycle with maximum amplitude (time 7.548 s) lead to a damping factor value of 2.43%, with respect o the critical one.

In Test SEIS-ULS relatively larger crack widths with respect to test SEIS-SLS was detected by the instruments, but the maximum values were nevertheless still very small, well within the limits for the SLS for static loading, albeit this was the ULS test. The maximum crack opening values reached among the instruments on the West side of the first floor slab were about 0.1 mm, and about 0.2 mm on the East side instruments.

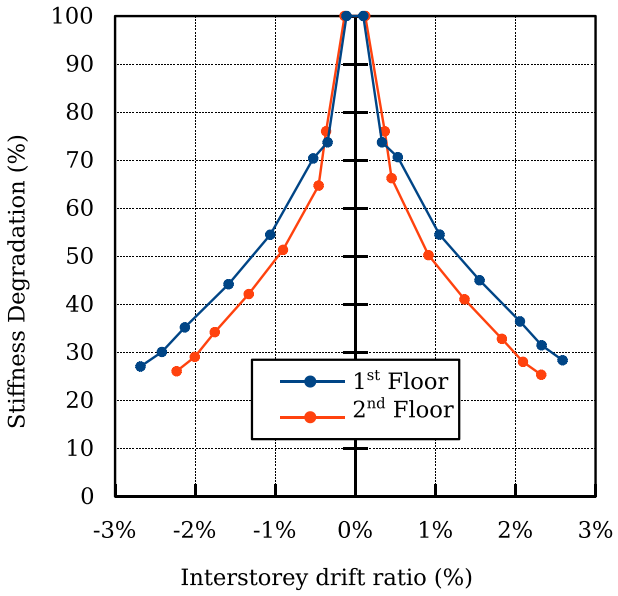

Fig. 15. Stiffness deterioration in Test CYC-1.

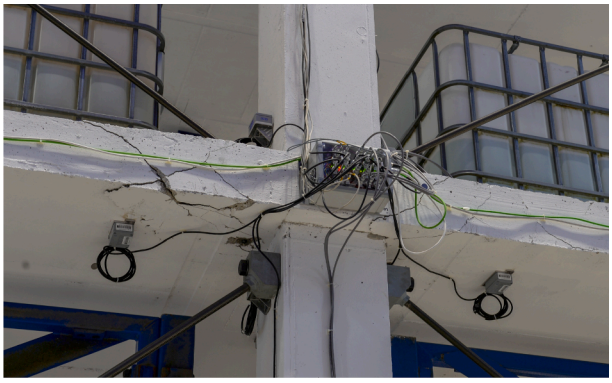

(a) Edge connections D2-1

(b) Corner connections D1-1 (short side)

Fig. 16. Edge and corner connections cracking at 2% drift ratio.

In the second floor slab the maximum values among West and East instruments were 0.02 mm and 0.04 mm, respectively. The substantial linearity of the response of the structure is very well highlighted in the final discussion, comparing the global response in the cyclic tests (see the next section) to the response here described.

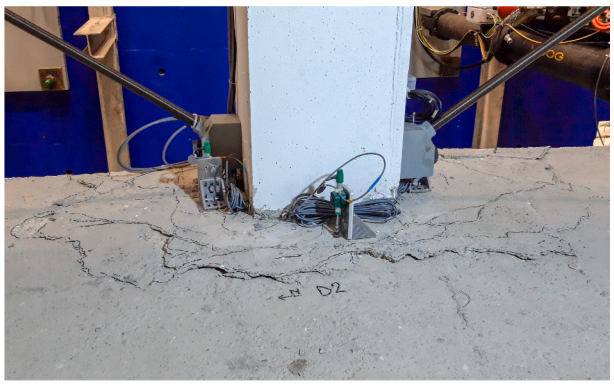

(a) Edge connections D2-1, top view

(b) Corner connections D1-1 top view

Fig. 17. Edge and corner connections cracking at 2.5% drift ratio.

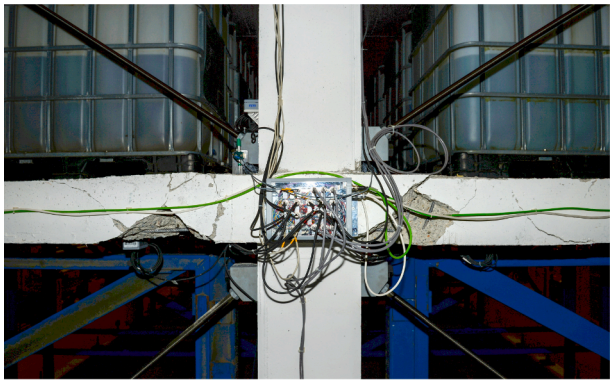

(a) Edge connections D2-1

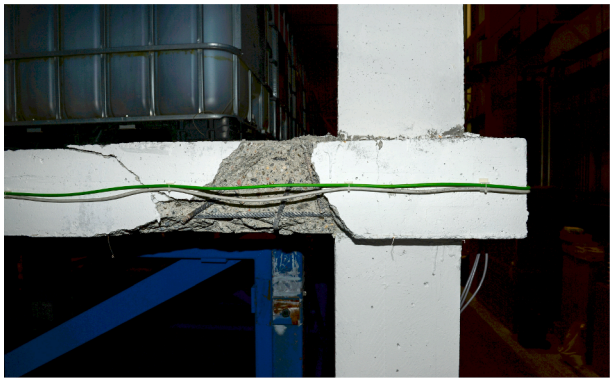

(b) Corner connections D1-1 (short side)

Fig. 18. Edge and corner connections, cracking after 2.5% drift ratio.

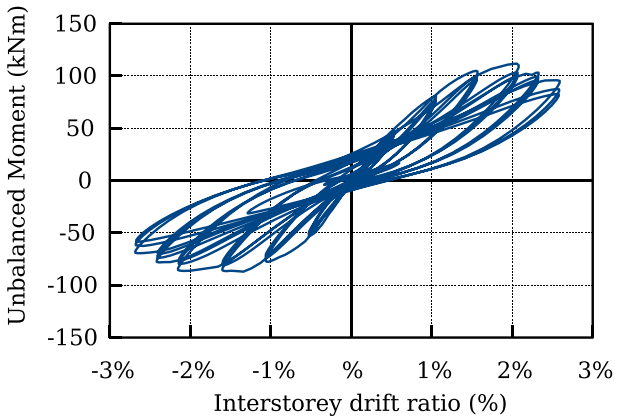

(a) Edge connection D2-1

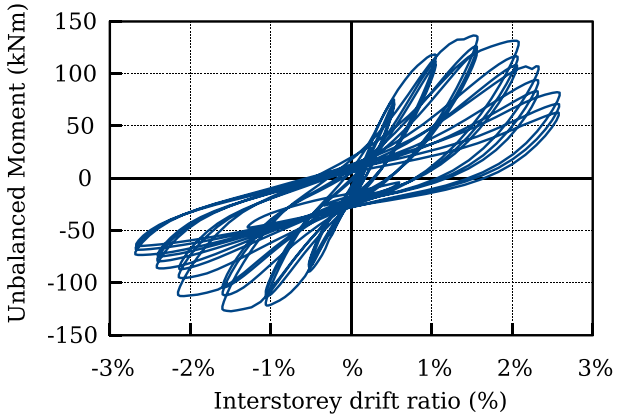

(b) Corner connection D1-1

Fig. 19. First floor, edge and corner connections diagrams of unbalanced moment and inter-storey drift ratio: D2-1 (a) and D1-1 (b).

6. Cyclic tests results

6.1. Cyclic test CYC-1 to 2.5% drift ratio

The global response is shown in Fig. 14a, in terms of total base shear, as the sum of all actuator forces, and the drift ratio of the second floor (top displacement divided by the total height of the building: 6300 mm), following the pattern in Fig. 7. Fig. 14b shows the relation of the sum of the two actuator forces at each storey to the interstorey drift ratio at each floor. The ratio of the actuator forces at the second and first storey was 2:1 and the displacement was controlled at the second floor. The first floor shows an increasingly higher interstorey drift ratio than the second floor. The maximum base shear is reached at 2% drift ratio. Beyond this level the 2.25% and 2.5% drift ratios were reached for nearly constant load. The first cycle for every drift ratio increase beyond 2% showed a very limited strength reduction. During the three cycles at each drift ratio level the strength deterioration was limited as well.

Fig. 15 presents for each floor the ratio between the secant stiffness in the first cycle, with a drift ratio of 0.25%, and the secant stiffness in the first cycle at each level of the drift ratio. The secant stiffness values are calculated using the force to interstorey drift ratio diagrams of Fig. 14b. The diagrams in Fig. 15 show a progressive loss of stiffness for both floors. The trend is similar for both the positive (East) and negative (West) loading directions. The second floor was provided with shear reinforcement; it showed limited stiffness deterioration at 0.5% drift ratio, followed by a trend similar to the first floor without shear reinforcement for higher lateral deformations.

The higher damage was in the edge and corner connections in the

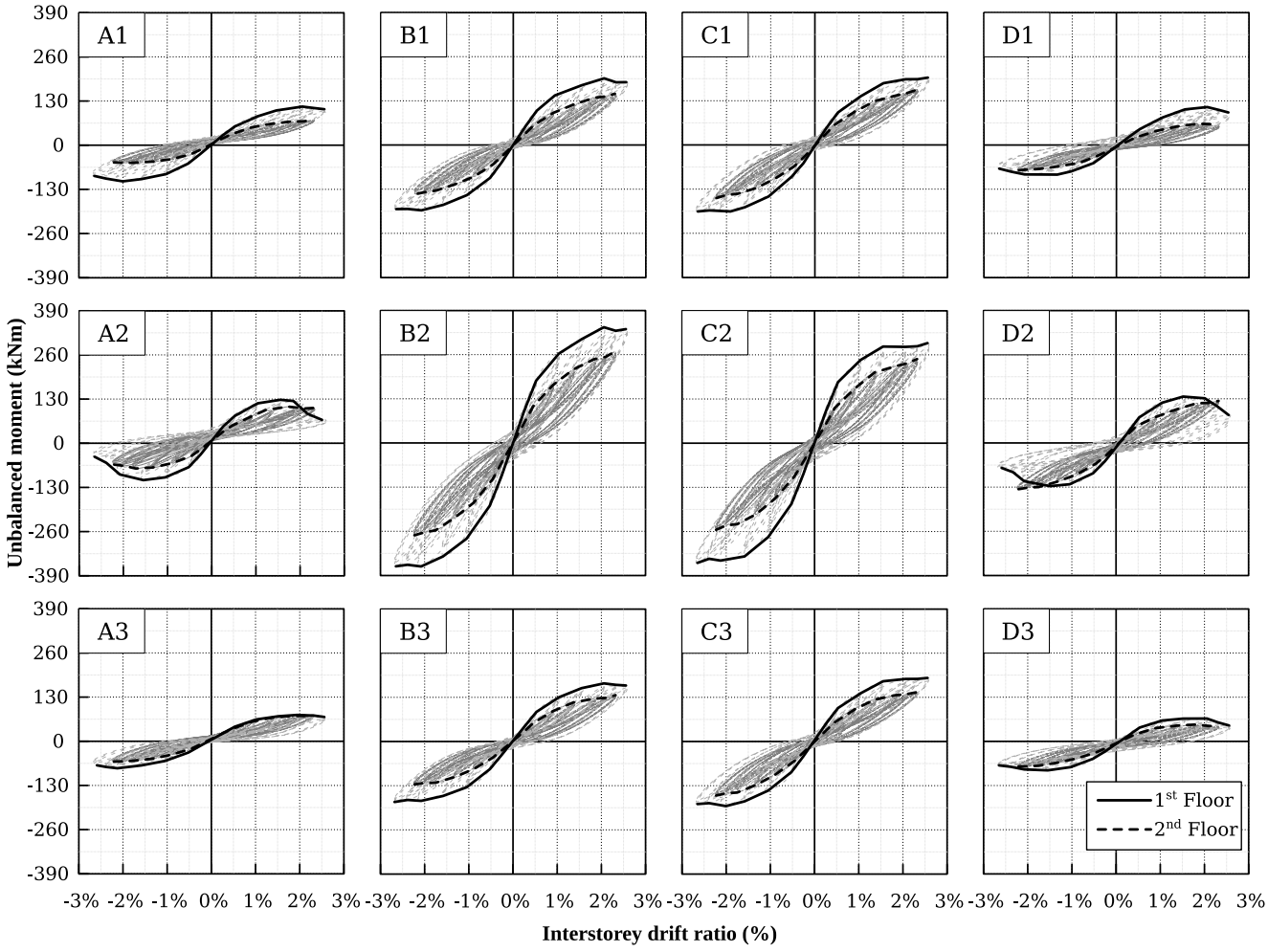

Fig. 20. Connection response in test CYC-1.

first floor along lines A and D orthogonal to the loading direction (Fig. 16). The most relevant cracks in the connections appeared on the vertical surface at the side of the slab. At 1.5% drift ratio a crack pattern of torsion and shear damage was clearly visible. The cracks opened wider at 2% drift ratio (Fig. 16) and and spalling of the concrete followed at 2.5% drift ratio (Fig. 17).

Observing the crack pattern, the failure mode is a combination of punching shear, with a cone reaching the top surface of the slab (Fig. 17) and torsion cracking in opposite diagonal directions on the side of the slab (Fig. 16). After the 2.5% test (Fig. 18) some portions of the spalled concrete around the connections were removed by hand, to avoid the falling of debris during the post-test measurement operations and the preparation of the following test. The failure cracks have an inclination of about 45° in agreement with the failure surfaces observed in slabs with similar amount of flexural reinforcement (whereas slopes of about 30° are more typical for slabs with significantly higher reinforcement ratios, see for instance [19], where slabs with different reinforcements in both reinforcements clearly show this effect).

The interior connections and the edge connections on the long side (parallel to the loading direction) in the first floor presented less damage. Similar considerations hold for the connections in the second floor with the transverse reinforcement.

The instrumentation provided the moment and shear in the columns; the unbalanced moment is calculated summing moments at the ends of columns framing into a connection. The first floor edge connections on both sides A and D (see detail for connections D1-1 and D2-1 in Fig. 19a) reached the maximum unbalanced moment at ±1.5% interstorey drift ratio. Starting from 2% drift ratio, the cycles were characterized by lower unbalanced moment on the first cycle and more significant strength and stiffness deterioration than the cycles at the previous drift ratio levels. The global response (Fig. 14a) was not affected by this local strength deterioration.

The unbalanced moment as a function of interstorey drift ratio for all connections is shown in Fig. 20. The strength deterioration of all connection along the A and D edges at the first floor is visible. A 20% reduction of the unbalanced moment, conventionally corresponding to failure, was reached for drift ratios higher than 2% in connections A2-1 (+2% and -2.1% drift ratio), D2-1 (+2.3% and -2.2% drift ratio), D1-1 (-2.6% drift ratio) and D3-1 (2.4% drift ratio). The internal and edge connections along line C and the internal connection B2-1 at the first floor show some increase in the unbalanced moment. The second floor connection present a stable response. The columns showed cracking and compression damage at the base of the first storey. No damage was observed in the sections above, at both storeys. Summing the moments developed at the base of the columns a value equal to approximately 1/4 of the total moment of the external jack forces is obtained.

6.2. *Strengthening of connections*

The seismic tests SEIS-SLS and SEIS-ULS caused very limited damage in the structure, as reported in Section 5. The following cyclic test CYC-1 damaged slab-column connections at the first floor, where no transversal reinforcement was placed. The damage was mainly along the short sides A and D of the specimen; the conditions were such (Fig. 16a) that no

(a) Strengthened interior connection C2-1

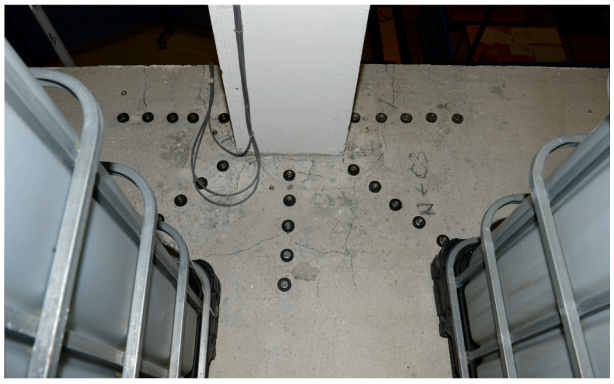

(b) Strengthened edge connection C3-1

Fig. 21. Strengthened slab-column connection at first floor: interior C2-1 (a) and edge C3-1 (b).

repair could be carried out. Therefore some of the slab-column connections along lines B and C were strengthened improving the punching-shear resistance, before the cyclic test CYC-2. This operation represents a realistic scenario, in which retrofitting is carried out after a major seismic event. The partial retrofit allows a direct comparison among the response of unreinforced connections, and those with post-installed and pre-installed shear reinforcement. Post-installed bolts were used in three connections in positions B1-1, C2-1 and C3-1. Bolts were placed into drilled holes across the slab thickness, reproducing the layout of headed-studs cast into the second floor slab. Threaded bars (8.8 steel grade) with 10 mm diameter were used, with rigid circular washers with 40 mm external diameter and 10 mm thickness. Nuts on both sides enabled to pre-load each bolt, ensuring the efficiency of the fastening. Fig. 21a and Fig. 21b show the strengthening of the interior connection (C2-1) and an edge connection (C3-1), respectively.

The strengthening was designed before the mock-up manufacturing, therefore small plastic tubes (4 mm diameter) were placed into the concrete slab in all the connections before casting, to ensure the positioning and verticality of drilled holes, avoiding any interference with longitudinal rebars and measuring devices. Nevertheless, the applicability of this technique for ordinary applications remains valid, it is only slower to perform and less precise for positioning. A rebar scanner may correctly locate existing reinforcement bars making the application more effective. The tubes did not alter the cracking pattern: during the surveys performed after each test, the radial cracks of the slab resulted not affected by the pre-holes. Once test CYC-1 ended, water tanks were removed from the first floor, both for practical reasons related to the installation and to reproduce the removal of non-structural loads, as would have been done for an intervention on a real building. The slabs were drilled, following the pre-holes, and the bolts were installed and tightened with a torque wrench to apply a preload of 10 kN. Finally, the water tanks for the additional loading and measuring instruments were positioned again.

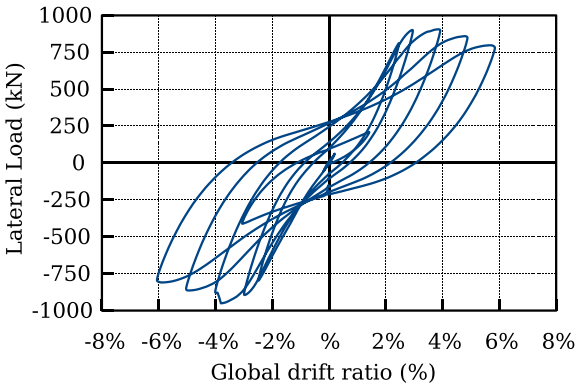

(a) Global lateral load – top floor drift ratio

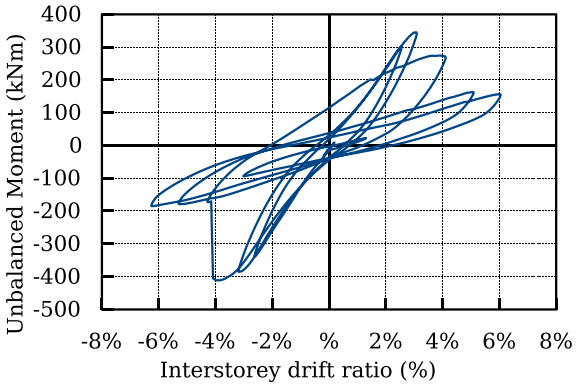

(b) Unbalanced moment to interstorey drift ratio diagram for connection B2 in the first floor slab.

Fig. 22. Test CYC-2: (a) Global lateral load vs. top floor drift ratio; (b) Unbalanced moment vs. interstorey drift ratio diagram for connection B2-1.

6.3. *Cyclic test CYC-2 to 6% drift ratio*

The severe damage reached in test CYC-1 along lines A and D at the first floor caused concern for the safety of the test. For the continuation of the activity the added loads were removed from half of the spans A-B and C-D. The remaining tanks were all filled at the same level (see Fig. 8c). Based on conventional calculations of the tributary areas, the gravity shear ratio of connection B2-1 was not significantly affected by the change in additional loads, while that of the connections along line C increased to reach the same GSR as line B. The second test showed an increase in lateral force for global drift ratios higher than 2.5%, up to -3.8% drift ratio where a punching failure occurred in the first floor slab at the interior slab-column connection B2-1. Fig. 22a shows the global base shear versus roof drift ratio relationship during the test. The structure had already entered a phase of plastic deformations during test CYC-1, with a horizontal plateau of the base shear force; nevertheless a slight increase of the base shear was observed during CYC-2. The global absolute maximum base shear of the two-storey specimen was reached, equal to -952 kN, for a roof displacement equal to -240 mm (3.8% global top storey drift ratio in the 4% cycle; 4% interstorey drift ratio for the first floor), when the punching of the interior connection occurred. After reaching the maximum base shear, a degradation of this quantity began and continued steadily until the end of the test at 62% horizontal drift ratio. The final global lateral force reduction was approximately 10%; part of this is due to the failure of the interior connection, part to the progressive deterioration of the connections on the short sides of the structure at the first and second floor, and part due to the second order effects. The test was stopped because the maximum stroke of the

(a) As-built interior slab-column connection B2-1

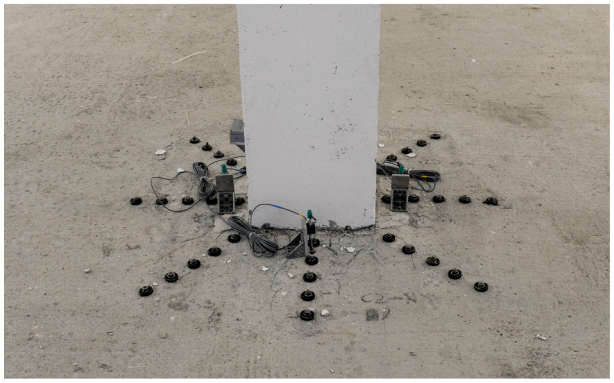

(b) Strengthened interior slab-column connection C2-1

Fig. 23. As-built (a) and strengthened (b) interior slab-column connections at end of test CYC-2.

actuators was reached. A post-test examination showed also the breaking of the longitudinal reinforcement at the base of the column in position B2.

The event that caused the onset of the global load reduction was the punching of connection B2-1 (Fig. 22a); after the two cycles at 2.5% and 3%, during the first cycle to -4% in the Westward direction the unbalanced moment dropped with a reduction of more than 50%; the response in the +4% half cycle showed significant strength deterioration as well; the cycles at 5% and 6% drift ratio show a post-peak response with low stiffness. The failure mode is evident observing the typical damage on the top slab surface around the column extending to a distance approximately up to 600 mm from the column face in all directions (Fig. 23a). The behaviour of the strengthened interior connection at C2-1 was significantly improved compared to the similar but not strengthened connection B2-1 (Fig. 24). The connection B2-1 degraded rapidly after punching, whereas the strengthened connection (C2-1) was able to survive to the end of the test, for nearly 6% storey drift ratio, without failure and limited damage showing on the slab surface (Fig. 23b). A similar performance was shown by the other two strengthened connections on the edges.

The edge connections B3-1 and C1-1 on the North and South sides with the edge parallel to the horizontal load did not fail, but showed some radial cracking around the columns and some damage in slab cross sections at the column face; the strengthening of connections B1-1 and C3-1 caused a more limited damage in these. The second floor (Fig. 24) had severe damage in the edge and corner connections along the East and West sides A and D; observing the unbalanced moment to drift ratio relations, the drift ratio corresponding to the maximum value for the unbalanced moment was equal of these connections was equal to 3%, followed by strength deterioration. A 20% reduction of the unbalanced moment, conventionally corresponding to failure, was reached at the first floor in connections A1-1 and A3-1, D1-1 and D3-1; at the at second floor, the failure was reached in connections A1-2, A2-2, A3-2, and D1-2 see Fig. 27b; D2-2 and D3-2 for drift ratios higher than 3%, see Fig. 27a. The damage in the slab was due to torsion on the North and South sides of the connections, with some cover spalling. Radial cracking was observed after the test around the interior connections and connections on the edges parallel to the loading. The connections that failed could still bear the gravity loads throughout test CYC-2 without the slab falling on the safety props. The slab longitudinal reinforcement with the Eurocode 2 [13] detailing rule with two bottom bars passing through the column was effective to this purpose. The observation of the structure after the tests suggests that also the top layer contributed: the top reinforcement was not debonded, and given the slope of the top surface that could be observed visually around the punched connections, all the reinforcement developed a catenary effect. The response of the column bases was important. A quarter of the moment of the lateral actions was balanced by the moments at the base. As previously mentioned, the breaking of tensile reinforcement at one column base, after compression buckling was observed after the end of the test. The columns reinforcement limited the cracking of these members that would have increased the ultimate drift ratio.

7. Discussions

The seismic and cyclic tests explored two different stages of the response. Fig. 25 shows the superposition of the response in the seismic ultimate limit state test SEIS-ULS and the cyclic test CYC-1. This comparison confirms that in the former test the flat slab frame response was nearly elastic, and that the design can take advantage of the nonlinear deformations with higher deformation capacity for the flat slab.

The global response in Fig. 25 and 26 confirms the capacity of flat slab frames to develop inelastic deformations with a stable response up to 2.5% drift ratio, for gravity shear ratios 0.2 and 0.3 in the interior connections. With part of the configuration changed in the second cyclic test CYC-2, still the results obtained provide insight on the continuation of the first test to higher drift ratios. Fig. 26 shows the response of the two cyclic tests in sequence. The repetition of the 2.5% global drift ratio cycle in test CYC-2 showed a response nearly identical to that of test CYC-1 at the same drift ratio. The interior connection B2-1 had GSR = 0.3 as in test CYC-1 and punched at 3.8% drift ratio. These results agree with the previous tests in the literature with similar gravity shear ratios, reaching ultimate drift ratios ranging between 2.5% and 6% [5].

The literature for scaled flat slab frames presents tests with different geometry, specimen design (seismic resistant or not), type of loading and reinforcement details [5]. Most studies used gravity shear ratios in the range 0.25–0.3 for interior connections, calculated using ACI318-14 (V_g/V_o) [20]; the values in the SlabSTRESS tests ranged 0.21÷0.29. The comparison with three studies without shear reinforcement and one with shear studs is discussed below. Tests by Hwang and Moehle [6,7] were carried out with biaxial loading. The prototype structure was designed as a part of a building with non-participating (secondary) slab. The gravity shear ratio was 0.3. In the first direction loaded (N-S) 4% global drift ratio was reached without loss of global lateral load resistance; edge joint failures occurred first and redistribution took place to the interior joints. Loss of lateral load capacity showed at 3.0% to 3.5% drift in the E-W direction. It can be stated that the redistribution of internal forces and the values of drift capacity are close to those occurring in tests CYC-1 and CYC-2. The differences are in the 40% scale of the test, the configuration with one floor and columns below the slab only and the biaxial loading. One cyclic tests on a scaled floor (50% of the prototype), with two by two spans and half columns above and below the slab was carried out by Rha et al. [8]. The interior connection punched first at 1.5% drift ratio, while the failures on the edges occurred progressively along the final loading to 5.7% drift ratio. The difference in the failure sequence could be explained by the higher gravity shear ratio on the interior connection (0.4), and all columns (interior, edge and corner) having the same square cross section dimensions; thus the

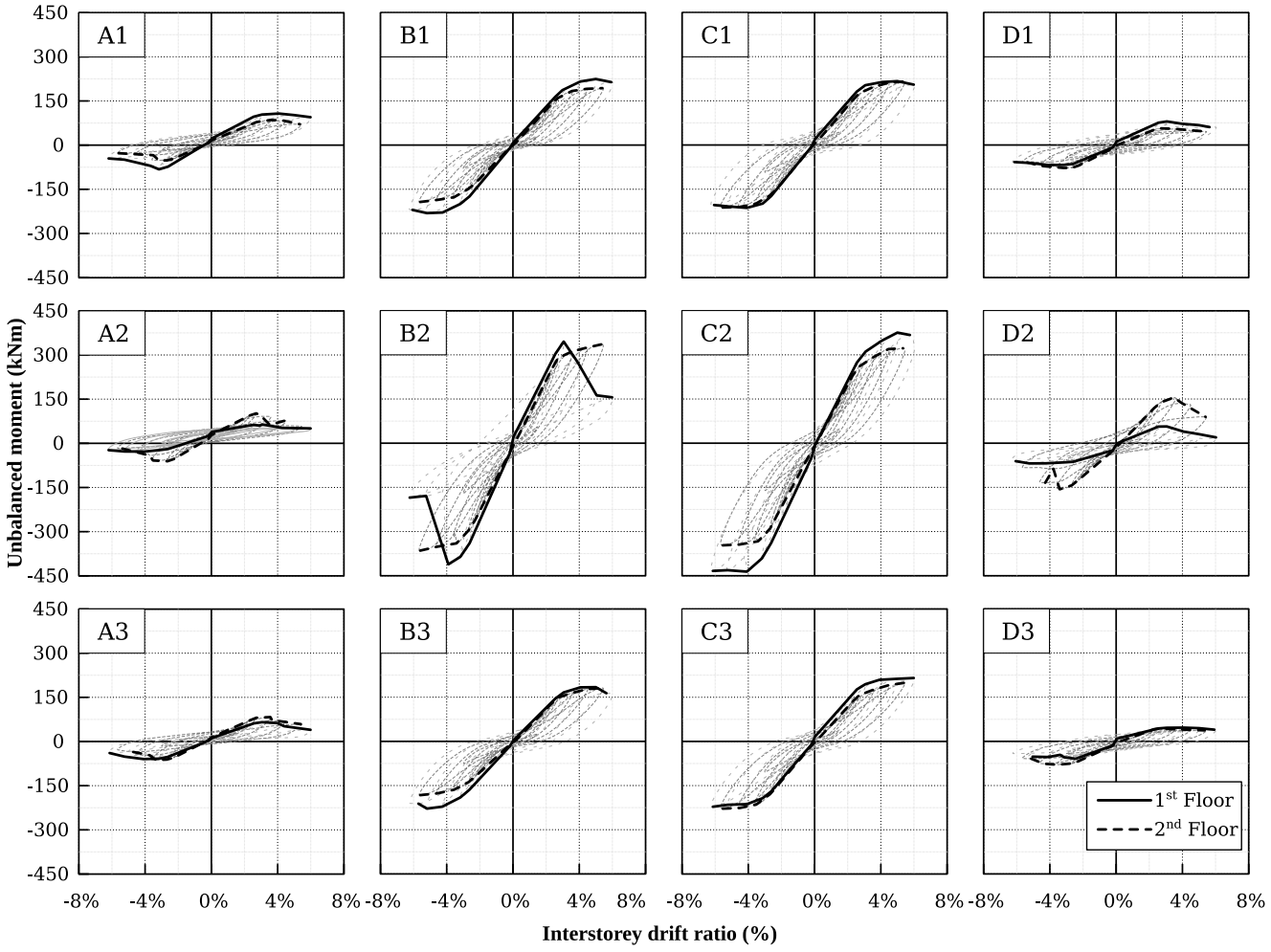

Fig. 24. Connection response in test Cyc-02.

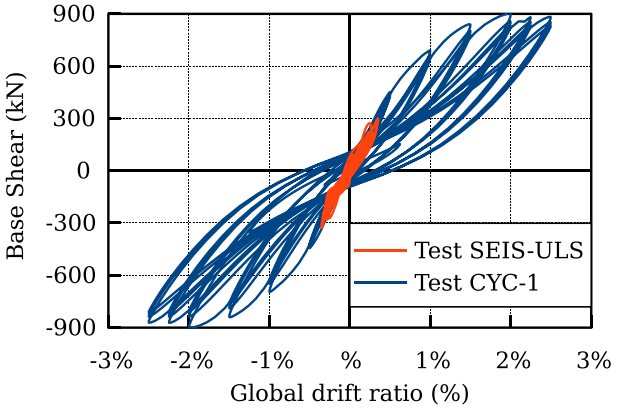

Fig. 25. Comparison of global response in seismic and cyclic tests.

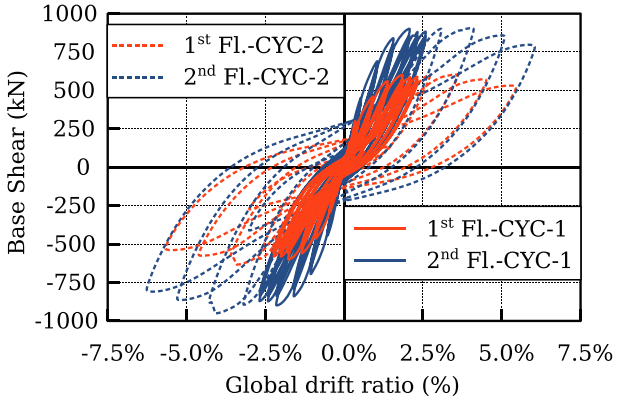

Fig. 26. Comparison of global response in tests CYC-1 and CYC-2, both at floor 1 and floor 2.

connections on the perimeter with lower gravity shear ratio showed a better performance. The global response on the whole agrees with the SlabSTRESS tests, showing the progressive failure of different groups of connections at different drift levels, up to a high drift ratio. One shaking table test was carried out by Moehle and Diebold [9] on a 30% scaled two storey primary flat slab frame with edge beams in the direction orthogonal to the lateral action. Drift ratios higher than 5% were reached with one interior connection showing a not fully developed punching failure at the end of the test. This test differed from the research presented here in the specimen design, the structural configuration and the reduced scale. Failures on the edges were prevented by the beams, though these were severely damaged. The interior connections still had a central role in the response up to high drift. Summing up, undoubtedly the literature presents cases with multiple differences, in addition to the scaled dimensions of the tests. The general conclusion is that the full-scale test results agree with the scaled tests in several aspects.

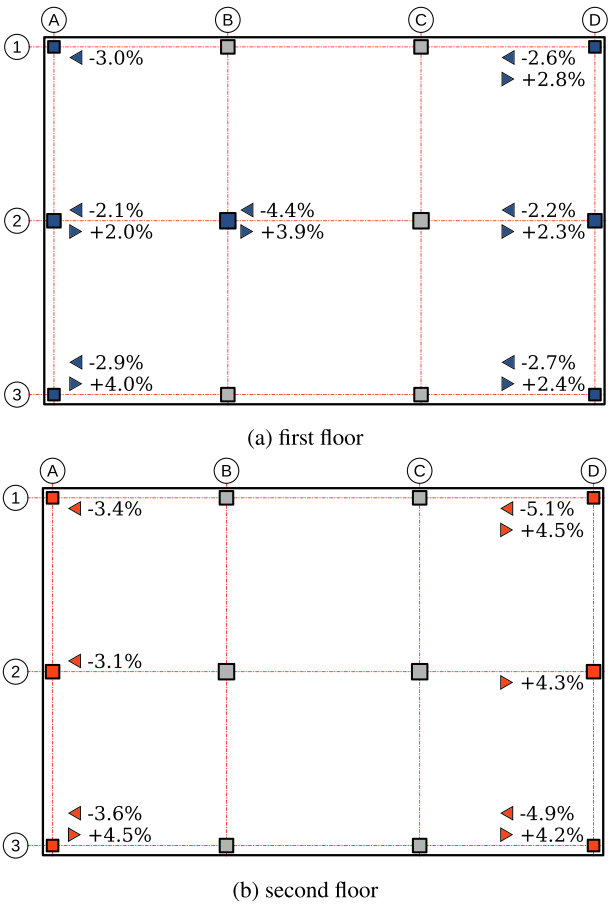

Fig. 27. Interstorey drift ratios at connection failure.

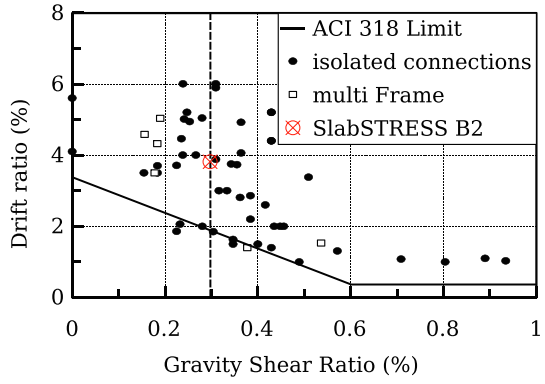

Fig. 28. Comparison of the result on internal connection with the database [4] of isolated and multi-frame connections.

A summary of the chord rotations of connections reaching failure is given in Figs. 27a and 27b, corresponding to the conventional 20% reduction of unbalanced moment. The interstorey drift ratios provide an approximation of the maximum slab rotation relatively to the column, confirmed by the experimental results.

Results for the ultimate drift capacity of connections in the literature (Pan and Moehle [16]; Megally and Ghali [21], Hueste et al. [2], Zhou and Hueste [3]; ACI-ASCE, 2015 [22]) report drift ratios at failure as a function of gravity shear ratios and failure modes. The comparison of the results of this campaign with a database of tests for isolated and multi-frame connections without shear reinforcement collected by Ramos et al. [4] is shown in Fig. 28. For interior connections at gravity shear ratio equal to 0.3 values range 2% to 6%. Tests reaching horizontal drifts of around 5% to 6% presented flexural, punching and mixed flexural/punching failures. The scatter in these results can be explained considering that these are influenced by several parameters, such as concrete strength, reinforcement ratio, ratio of slab thickness to column dimensions and slab slenderness. Also different boundary conditions and testing schemes were used. The B2-1 connection ultimate drift result is close to the mean of the test results with the same gravity shear ratio. The C2-1 connection did not fail up to 2.5% drift ratio for gravity shear ratio equal to 0.2, in accordance with the lower bound of the ACI318-14 limit [20]. The two connections on the edges parallel to lateral load without strengthening did not fail up to 6% drift ratio, for a gravity shear ratio equal to 0.21. Hence for these types of connections the tests results are broadly in accordance with the existing results on isolated and smaller scale specimens. Concerning the connections with shear reinforcement, the existing results in the literature for isolated interior connections (e.g. Hueste et al. [2]; Megally and Ghali [21]) show a sizeable increase of ultimate drift ratios, with values above 6% for GSR = 0.3. The only flat slab frame with shear reinforcement tested by Kang and Wallace [10,11] showed lower ultimate drift ratios in the connections between 2.5% and 3.35% with GSR = 0.3 possibly due to the loss of shear capacity at the slab-column interface, and the most significant damage in the edge connections. The tests carried out here for the interior and edge (parallel to the load) connections with studs and with post installed strengthening suffered limited damage up to 6% drift ratio, in agreement with the literature for interior connections referenced above. The testing program aimed to increasing the knowledge also for the edge and corner connections with lateral actions orthogonal to the edge, with a limited number of tests in the literature. These reached failure between 2% and 4.4% drift ratio without shear reinforcement, and 3.1% to 5.1% interstorey drift ratio with shear studs. Hence the increase of ultimate drift ratio with shear reinforcement was sizeable, though the edge and corner connections showed lower ultimate drift ratios with respect to interior connections. This result at both floors was influenced by the anchorage detail with a simple bend of the longitudinal reinforcement on the free edges. The detail was used because of the common use in European practice, and the interest to study the response of existing structures. The efficiency of other edge details requires more research. One of the aims of the testing campaign was to explore the redistribution of internal load effects; this is confirmed for both CYC-1 and CYC-2 tests by the connections response in Fig. 20 and 24 from the short edges to the internal connections and to the edges parallel to the loading. The efficiency of the applied strengthening solution was demonstrated in test CYC-2, with the good conditions of the three strengthened connections after the 6% drift ratio test. A similar performance was indicated by tests on isolated connections (Almeida et al. [23]). The tests provide indications on post critical conditions, showing that the given gravity loads could still be supported with the longitudinal reinforcement provided, in the connections without shear reinforcement or strengthening. As mentioned at the beginning of this section, the results of the real scale test carried out confirm the possibility to take into account the development of nonlinear deformations in the design of flat slabs – a result of the studies on isolated connections and scaled flat slab frames (Coronelli et al. [5]). The research developments will deepen into the local response measured for the connections, considering the two different longitudinal reinforcement ratios, the detailing and the use of shear reinforcement, in order to provide indications for the design.

8. Conclusions

Full-scale testing was carried out on a two storey flat-slab frame with gravity and lateral loading, including the seismic and cyclic response up to ultimate conditions. The research achieved a detailed description of the behaviour of the structure throughout the different types of tests and phases of the response, at a global and local scale. The global seismic response has been verified by pseudodynamic testing with virtual walls,

showing very limited damage up to seismic excitation compatible with the ultimate limit state spectrum. The research developments are open to the calibration of models based on the measured response, and the prediction of the combined behaviour of walls and flat slab frames The cyclic response was measured with the frame response to ultimate conditions involving the failure of several connections in a sequence. A global ultimate drift ratio higher than 2.5% is reported, with connection failures between 2% and 3.8% interstorey drift ratio. After strengthening some of the connections on the first floor, a global drift ratio of 6% was reached with a limited lateral force reduction. Redistribution of load effects and different types of failures in the connections were shown. At a global scale the results confirm the ultimate deformation capacity of flat slab frames shown in the literature [5]. Comparing the results of ultimate drift capacity of the connections, values comparable and higher than those in databases in the literature were measured. The results extend the knowledge in the literature based mainly on isolated connections and/or reduced scale specimens, because a real scale scale structure was investigated. The tests showed the importance of the damage and failure in edge and corner connections. These results are valuable for the study of existing structures, because the configuration studied has been frequently used in Europe. The effect of different reinforcement details along the edges requires more investigation. The response of one floor with no transverse reinforcement and one with welded shear studs was compared. The performace of the latter was better, with higher ultimate drift ratio for edge and internal connections. The comparison of the two configurations will be the object of future studies. Strengthening of a set of connections was carried out after a first level of damage was reached using post-instaled shear bolts, and the efficient performance of the system for higher drift ratios was shown.

Declaration of Competing Interest

The authors declare that they have no known competing financial interests or personal relationships that could have appeared to influence the work reported in this paper.

Acknowledgements

The experimental campaign is part of the Transnational Access activities of the SERA project (Seismology and Earthquake Engineering Research Infrastructure Alliance for Europe). This project has received funding from the European Union's Horizon 2020 research and innovation programme under grant agreement No.730900.

Appendix A. Pseudodynamic test

The response of the SlabSTRESS model to the specified accelerogram was obtained in the ELSA laboratory by solving the equation of motion (1):

$$\mathbf{M}\ddot{\mathbf{d}}(t)+\mathbf{r}(t)=-\mathbf{M}\cdot\mathbf{I}_g\cdot a_g(t) \tag{1}$$

using in vector $\mathbf{d}(t)$ two DoFs for the longitudinal displacements at the floors and the respective restoring forces being $\mathbf{r}(t)$. The right hand side of the equation represents the inertial forces, obtained by multiplying the ground acceleration by the theoretical mass matrix and the incidence vector of the earthquake $\mathbf{I}_g$. The pseudo-dynamic (PsD) method with substructuring was used for solving Eq. (1) in terms of relative displacements to the ground. The method is called PsD, or hybrid, when the real (experimental) time is much larger than the prototype time used in the equation of motion (1). It means that the inertial forces that appear in the equation need to be computed numerically (through a theoretical lumped mass matrix $\mathbf{M}$ in this case) since they cannot be measured in the (quasistatic) experiment. This technique is a hybrid testing method that combines restoring forces measured on a physical substructure with restoring forces coming from a numerical substructure.

$$\mathbf{r}(t)=\mathbf{r}_n(t)+\mathbf{r}_p(t) \tag{2}$$

The restoring forces coming from the shear walls were simulated numerically, whereas the restoring forces were measured from the physical specimen when submitted to the solved displacements. The mass of the walls ($\mathbf{M}_N$) was considered within the matrix, together with the mass of the physical structure ($\mathbf{M}_P$): ($\mathbf{M}=\mathbf{M}_N+\mathbf{M}_P$). An evolved version of the continuous PsD method developed at ELSA (Molina et al. [24] was used for this tests. Using such method, every original time increment of the accelerogram (0.005s) in this case) is subdivided in a high number of sub-steps (2000 in this case) and, at each sub-step, the physical forces are measured, whereas the numerical ones are computed, and the next displacements are solved and imposed to the specimen. Every sub-step is performed in one sampling period of the real-time controller (1 ms currently). This is possible for the controller used whenever the numerical model consists of constant matrices of stiffness and viscous damping. As explained in a more comprehensive manner by Pegon et al. [25], this particular algorithm strategy is called monolithic substructuring since both substructures use the same time discretisation in a common solving algorithm (Explicit Newmark in our case). Considering that the prototype time increment of every sub-step of the accelerogram was 0.005s/2000 $= 2.5\times10^{-6}$s, being executed in 1ms of real time, it can be said that the experiment was performed with a time dilation of 1×10^{-3}s/2.5×10^{-6}s $=400$. As usually it is done in ELSA, the equivalent damping distortion introduced in the response by the control errors was assessed and shown to be negligible so that the quality of the results was not affected by them. The special technique for performing such assessment from the experimental results is described by Molina et al. [26], while more details about the controller are given in Peroni et al. [27].

Since it was required to numerically simulate the walls using a linear model, an equivalent linear model of the walls was used for both tests SEIS-SLS and SEIS-ULS. The related properties (described through a stiffness and a damping matrix) were derived from the response of a nonlinear model of the walls [28] implemented inside the research computer code NONDA (Martinelli et al. [29]). From the non linear dynamic time history simulations under the above mentioned ground motions it was discovered that, although the structure mainly responds in its first mode, during both ground motions it changes its stiffness and damping in a significant way, reaching a drift ratio at the top up to about 0.6% which is well beyond the cracking in tension of concrete and slightly larger than yielding of bending reinforcement. Hence a compromise linear model was selected that maximized the fit with the nonlinear response of the walls in the strong part of the accelerogram.

References

[1] Pinto A, Taucer F, Dimova S. Pre-Normative Research Needs to Achieve Improved Design Guidelines for Seismic Protection, Technical Report, JRC, 2007. URL: https://eurocodes.jrc.ec.europa.eu/doc/EUR22858EN.pdf.

[2] Hueste MBD, Browning J, Lepage A, Wallace JW. Seismic design criteria for slab-column connections. ACI Structural Journal 2007;104(4):448–58. https://doi.org/10.14359/18775.

[3] Zhou Y, Hueste MBD. Review of test data for interior slab-column connections with moment transfer, vol. 2016-October, American Concrete Institute, ACI Special Publication, Fédération internationale du béton (fib) and American Concrete Institute (ACI), 2017, Farmington Hills, MI 48331–3439 USA, 2016, p. 141–166. https://doi.org/10.35789/fib.bull.0081.ch08.

[4] Pinho Ramos A, Marreiros R, Almeida A, Isufi B, Inácio, M. Punching of flat slabs under reversed horizontal cyclic loading, vol. 2016-October, American Concrete Institute, ACI Special Publication, Fédération internationale du béton (fib) and American Concrete Institute (ACI), 2017, Farmington Hills, MI 48331-3439 USA, 2016, p. 253–272. https://doi.org/10.35789/fib.bull.0081.ch13.

[5] Coronelli D, Muttoni A, Pascu IR, Pinho Ramos A, Netti T. A state of the art of flat-slab frame tests for gravity and lateral loading. Struct Concr 2020;21(6):2764–81. https://doi.org/10.1002/suco.202000305.

[6] Hwang S-J, Moehle JP. An experimental study of flat-plate structures under vertical and lateral loads, Technical Report, 1993. URL: https://nisee.berkeley.edu/elibrary/Text/238467.

[7] Hwang S-J, Moehle JP. Vertical and lateral load tests of nine-panel flat-plate frame. ACI Struct J 2000;97(1):193–203. https://doi.org/10.14359/849.

[8] Rha C, Kang TH-K, Shin M, Yoon JB. Gravity and lateral load-carrying capacities of reinforced concrete flat plate systems. ACI Struct J 2014;111(4):753–64. https://doi.org/10.14359/51686731.

[9] Diebold JW, Moehle JP. Experimental Study of the Seismic Response or a Two-Story Flat-Plate Structure, Technical Report, Earthquake Engineering Research Centre, 1984. URL: https://nehrpsearch.nist.gov/static/files/NSF/PB86122553.pdf.

[10] Kang TH-K, Wallace JW. Dynamic responses of flat plate systems with shear reinforcement. ACI Struct J 2005;102(5):763–73. https://doi.org/10.14359/14672.

[11] Kang TH-K, Wallace JW. Punching of reinforced and post-tensioned concrete slab-column connections. ACI Struct J 2006;103(4):531–40. https://doi.org/10.14359/16429.

[12] Fick DR, Sozen MA, Kreger ME. Response of full-scale three-story flat-plate test structure to cycles of increasing lateral load. ACI Struct J 2017;114(6):1507–17. https://doi.org/10.14359/51689502.

[13] EN 1992-1-1: Eurocode 2: Design of concrete structures - part 1–1: General rules and rules for buildings, 2004.

[14] EN 1998-1: Eurocode 8: Design of structures for earthquake resistance – Part 1: General rules, seismic actions and rules for buildings, 2004.

[15] Aggiornamento delle norme tecniche per le costruzioni, 2018. URL: https://www.gazzettaufficiale.it/eli/gu/2018/02/20/42/so/8/sg/pdf, [in italian].

[16] Pan A, Moehle JP. Lateral displacement ductility of reinforced concrete flat plates. ACI Struct J 1989;86(13):250–8. https://doi.org/10.14359/2889.

[17] Drakatos IS, Muttoni A, Beyer K. Mechanical Model for Drift-Induced Punching of Slab-Column Connections without Transverse Reinforcement. ACI Struct J 2018;115(2):463–74. https://doi.org/10.14359/51701110.

[18] ACI 421.2R-07: Seismic Design of Punching Shear Reinforcement in Flat Plates, 421.2R-07, Farmington Hills, MI 48331-3439 USA, 2007. URL: https://www.concrete.org/publications/internationalconcreteabstractsportal/m/details/id/18565.

[19] Sagaseta J, Muttoni A, Ruiz MF, Tassinari L. Non-axis-symmetrical punching shear around internal columns of RC slabs without transverse reinforcement. Mag Concrete Res 2011;63(6):441–57. https://doi.org/10.1680/macr.10.00098.

[20] ACI CODE 318-14: Building Code Requirements for Structural Concrete and Commentary, Farmington Hills, MI 48331-3439 USA, 2014. URL: https://www.concrete.org/store/productdetail.aspx?ItemID=318U14.

[21] Megally S, Ghali A. Punching shear design of earthquake-resistant slab-column connections. ACI Struct J 2000;97(5):720–30. https://doi.org/10.14359/8807.

[22] Joint ACI-ASCE Committee 421, Guide to Seismic Design of Punching Shear Reinforcement in Flat Plates, ACI, Farmington Hills, MI 48331, 2010.

[23] Almeida AFO, Alcobia B, Ornelas M, Marreiros R, Pinho Ramos A. Behaviour of reinforced-concrete flat slabs with stirrups under reversed horizontal cyclic loading. Mag Concrete Res 2020;72(7):339–56. https://doi.org/10.1680/jmacr.18.00209.

[24] Molina F-J, Verzeletti G, Magonette G, Buchet P, Renda V, Geradin M, et al. Pseudodynamic tests on rubber base isolators with numerical substructuring of the superstructure and strain-rate effect compensation. Earthquake Engng Struct Dyn 2002;31(8):1563–82. https://doi.org/10.1002/eqe.176.

[25] Pegon P, Molina F-J, Magonette G. Continuous pseudo-dynamic testing at ELSA. In: Saouma V, Sivaselvan M, editors. Hybrid Simulation Theory, Implementation and Applications. Taylor & Francis; 2008. p. 79–88. https://doi.org/10.1201/9781482288612.

[26] Molina F-J, Pegon P, Poljansek M, Taucer F. Advanced reliability method applied to a hybrid seismic test of a retrofitted motorway bridge, 16th World Conference on Earthquake Engineering, 2017. URL: https://www.wcee.nicee.org/wcee/article/16WCEE/WCEE2017-1953.pdf.

[27] Peroni M, Molina F-J, Pegon P, Buchet P. Ethernet-based servo-hydraulic real-time controller and DAQ at ELSA for large scale experiments. J Earthq Eng 2021. Accepted by the Journal, in publishing.

[28] Martinelli L. Modeling shear-flexure interaction in reinforced concrete elements subjected to cyclic lateral loading. ACI Struct J 2008;105(6):675–84. https://doi.org/10.14359/20095.

[29] Martinelli L, Mulas MG, Perotti F. The seismic response of concentrically braced moment-resisting steel frames. Earthquake Engng Struct Dyn 1996;25(11):1275–99. https://doi.org/10.1002/(SICI)1096-9845(199611)25:11<1275::AID-EQE616>3.0.CO;2-U.